State Space Model, Controller Design Method and FEM based Verification of V-Shaped Electrothermal Microactuator

Muhammad Umar Masood * Javed Akhtar † Erick G. Moreno ‡

This paper presents the dynamic state space model for the v-shaped beam electrothermal microactuator, with state space representation. Voltage difference applied on the ends of the V-shaped beams, and the external load is taken as input, while the displacement of the shuttle is output of the dynamic system. There is only one state of the system defined, which is the change in temperature in the structure. Step and sinusoidal response of the system is studied along with the discussion on its dynamic performance. A control design technique is also developed and demonstrated by applying a Linear Quadratic Regulation on the electrothermal microactuator, fulfilling all the design constraints of fabrication process. The dynamic model is validated by a Finite Element Method electro-thermo-mechanical multi-physical model, by comparing the step response of both models. It is shown that the controller can pace up the time response of this microactuator which is traditionally known to have slower response as compared to others. The response can be increased by more than 10 times. The dynamic limitations of the microactuator are also studied.

I. Introduction

The constant miniaturization of electrical systems and electronics is essential to maintain the $200B Integrated Circuit (IC) industry afloat[1] . This industry is the responsible of many products that changed the world and society's dynamics e.g. personal computers, cellphones, sensors, instrumentation. One crucial part within this radical change are the microelectromechanical systems (MEMS). MEMS are integrated systems that consist of microelectronics (IC), microactuators and, in some cases, microsensors.[2] Thus, by improving one of these elements, MEMS would perform better and, subsequently, the concerning devices too. Besides, it could open up many unexploited fields, e.g. optics, transportation and medical engineering[3] which are mainly limited by the microactuator component.
Microactuators are devices that convert a form of energy into mechanical work at a microscale.They are still considered to be primitive[3] ; there is a constant trade off between parameters such as the range of motion, precision, force and power consumption that constrain their application.[4]
There exist various types of microactuators which are typically categorized depending on the form of energy (e.g. thermal, electrical, electromagnetic, electrostatic[4,5]) that is used to produce the work. Within the electrothermal actuators, the motion is produced by thermal expansion, typically induced by Joule heating effect which generates a temperature difference.[1,4] This particular type of microactuator is a promising alternative whenever large displacement and low-power MEMS actuators are required. Some of the most common applications are: extremely precise medical instrumentation, micro-relays and tunable impedance RF networks.[6] There are three fundamental geometries that are employed for the electrothermal microactuator. The U-shaped beam which is capable of generating circular motion (Arc); the Z- and V-shaped beams which can generate only rectilinear displacements.[7] The facts that the Z- and V-shaped microactuators are intrinsically symmetric,therefore, more stable; not to mention that rectilinear displacement is preferred for a wider range of MEMS applications[7] makes these two configurations more attractive. Nonetheless, after an extensive analysis conducted by Zhang et al.,[8] it was concluded that V-shaped are superior to Z-shaped microactuators for most of the cases. The V-shaped microactuator consists of an arrangement of parallel V-shaped (inclined) "beams" attached to a central body, called "shuttle". The beams are constrained and therefore any (heat) load that is applied to it will tend to manifest at the "free" end, which is where the shuttle

*Graduate student, Department of Mechanical and Aerospace Engineering, New Mexico State University at Las Cruces, New Mexico, USA. umar@nmsu.edu

†Graduate student, Department of Mechanical and Aerospace Engineering, New Mexico State University at Las Cruces, New Mexico, USA. akhtarj@nmsu.edu

‡Graduate student, Department of Mechanical and Aerospace Engineering, New Mexico State University at Las Cruces, New Mexico, USA. emorenor@nmsu.edu

is located. In other words, any compression/tension is subjected to will produce linear displacement parallel to the axis of symmetry of the microactuator (See Figure 3).
After extensively going through the state of art of microactuators, the lack of state-space modeling became evident. The well-known advantages of stating the system in this form are the motivation for developing it, we believe that this contribution will enhance and facilitate the analysis of microactuators allowing better designs. Furthermore, as per the best of the knowledge of author, no explicit controller design has been given for electrothermal actuators. The implementation of the state-space modeling (relating inputs to outputs) will become a tool to be able to design specific controllers depending on the desired application.

II. Governing Equations and Dynamic Modeling

A. General Modeling

Electrothermal microactuator works on the principle of Joule heating which happens because of the current passing through the structure, as a result of applied voltage difference on the extreme ends. Having the temperature rise in the structure, the beams expand and cause the center shuttle to move in the forward direction. This system combines the electro-thermo-mechanical coupled field modeling, which can be decomposed into two sub-models Fig. 1. For the electrothermal sub model, temperature rise is an output for a corresponding input of voltage. This sub model contribute to the dynamic behaviour of the actuator. The other sub model has two inputs, the temperature rise in the structure and the external load or the reaction force applied on the shuttle from the environment. The output of this sub model is the displacement of the shullte. Fig. 1 shows the block diagram of the dynamic model of the system. It has been shown in previous work that overall dynamic response of the system is dominated by

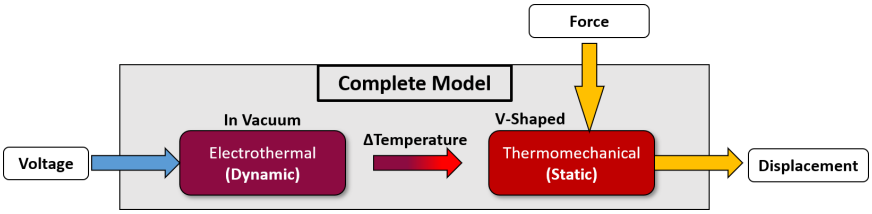

Figure 1. General Model

electrothermal response. Therefore, the mechanical inertia is considered to be quasi-static and thermomechanical modeling is considered in static level for our work.

B. Electrothermal Modeling

The beams employed in the micro-actuators are thin enough to assume 1-D heat transfer. The present model only considers joule heating in vacuum; therefore, the only non-negligible heat transfer mode is conduction. The equation that describes the sudden change of temperature of the micro-actuator is the unsteady-state conduction equation. See (1).

$$\rho C_p \frac{\partial u}{\partial t} - k \frac{\partial^2 u}{\partial x^2} = \dot{q} \tag{1}$$

By dividing the entire equation by the volumetric heat capacity (ρC_p), a more convenient form of (1) is obtained as (2). The volumetric heat capacity term simply tells how much heat is needed to increase the temperature by one unit per unit of volume.

$$\frac{\partial u}{\partial t} - \hat{k} \frac{\partial^2 u}{\partial x^2} = \dot{f} \tag{2}$$

Where $\hat{k} = k/(\rho C_p)$ and $\dot{f} = \dot{q}/(\rho C_p)$. $\hat{k}$ is called the thermal diffusivity, it is a measure of how fast the heat is diffusing through the material. In the other hand, $\dot{f}$ is the corresponding temperature.

The Volumetric heat generation ($\dot{q}$) is entirely governed by the Joule heating effect. This heating can be computed by finding how much of the electric current is converted (lost) into heat as it flows through the material. The higher the current resistance, the higher the heat gained. The system was therefore simplified as follows. In Figure (2), for a single unit (consider beam-shuttle-beam structure as one unit), the electrical resistances can been

seen connected in series and m number of such units are connected in parallel. Hence the total resistance of actuator is:

$$R = \frac{1}{m}(2R_b + R_s) \tag{3}$$

$$R_b = \hat{\rho}\frac{L_b}{A_b},\ R_s = \hat{\rho}\frac{L_s}{A_s}$$

Where, R is total resistance of actuator, m is number of the units, L_b and L_s are the length of the beams and shuttle respectively and $A_b(= W_b t)$ and $A_s(= W_s t)$ are the cross-sectional area of the beams and shuttle (See Figure 3). If the voltage supply across the actuator is U, then heat generation q because of joule-heating is

$$q = \frac{U^2}{R} \tag{4}$$

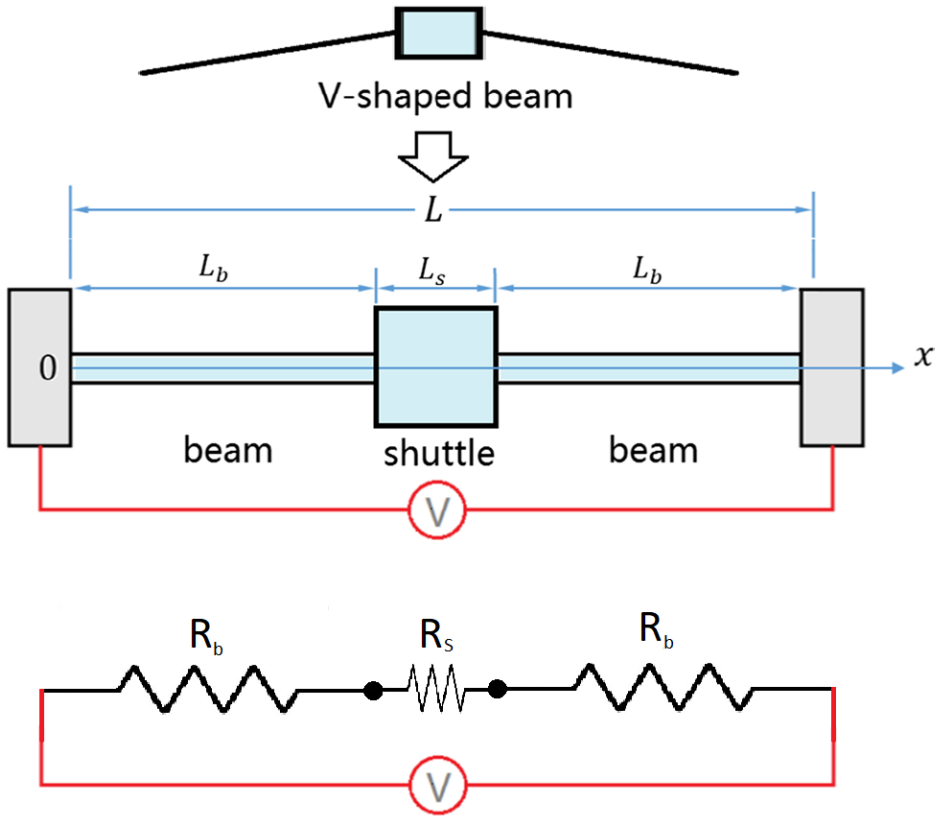

Figure 2. Electrical resistance diagram of the V-shaped actuator

Thus, Volumetric heat generation rate $\dot{q}$ can be written in the form of

$$\dot{q} = \frac{A_b A_s}{\hat{\rho}(2L_b A_s + L_s A_b)(A_b L_b + A_s L_s)} U^2 \tag{5}$$

By scanning the problem, it is noted that the heat transfer, and, therefore, the temperature distribution can be separated into two parts: the steady-state and the transient-state part. The total punctual temperature will be a result of the algebraic sum of the two previously mentioned parts (6). When substituing (6) into (2), two separate equations are obtained. One ODE, for the steady-state part (7), and, one PDE, for the transient part(8). These two equations are to be solved with the Boundary Conditions (BC) and Initial Conditions (IC) for the micro-actuator. (See Table 1).

$$u(x,t) \ = \ w(x) \ + \ v(x,t) \tag{6}$$

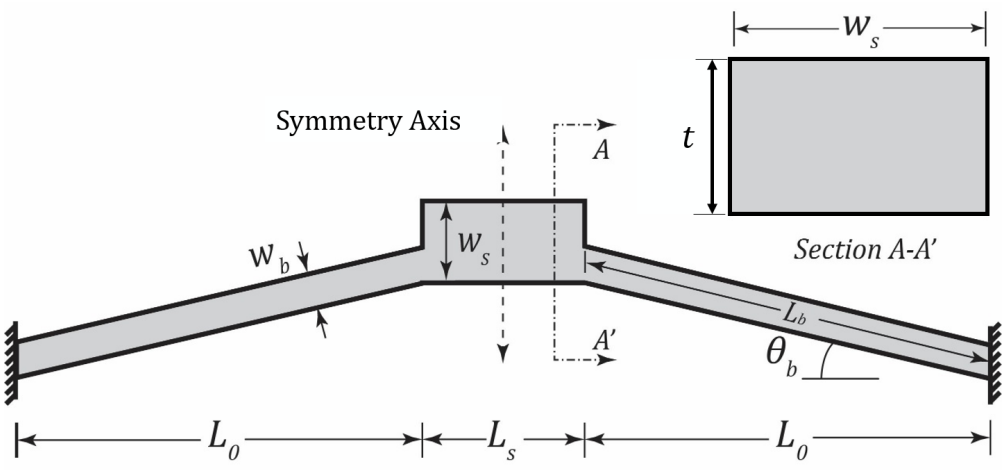

Figure 3. V-shaped geometry notation

$$\frac{d^2w}{dx^2} = -\frac{\dot{f}}{\hat{k}} \tag{7}$$

$$\frac{\partial v}{\partial t} - \hat{k}\frac{\partial^2 v}{\partial x^2} = 0 \tag{8}$$

To solve the steady-state part, solving the ODE (7) by integration with respect to x, and using the boundary conditions is required. The outcome (9) is a function that describes the punctual temperature due the steady-state.

$$w(x) = -\frac{\dot{f}}{2\hat{k}}x^2 + \frac{\dot{f}L}{2\hat{k}}x + T_0 \tag{9}$$
$$where,\ L = 2L_b + L_s$$

For the transient-state part, the most-common procedure is separation of variables (SOV). The assumption is that the general solution (10) can be decomposed into two ODE's: one ODE for the dimensional part (11) and the another one for the temporal part (12).

$$v(x,t) = X(x)T(t) \tag{10}$$

$$\hat{k}X'' + \lambda X = 0 \tag{11}$$

$$T' + \lambda T = 0 \tag{12}$$

Table 1. Boundary and initial conditions for actuators

	u(x,t)=w(x)+v(x)		
	u(x,t)	w(x)	v(x,t)
B.C.			
x=0	$u_0 = T_0$	$w_0 = T_0$	$v_0 = 0$
x=L	$u_L = T_0$	$w_L = T_0$	$v_L = 0$
I.C.			
t=0	$u=T_0$	w	$v = T_0$ - w

The two ODE's are also to be solved with the boundary conditions to later be combined into a unique solution that will give the punctual temperature corresponding to the transient-part. This procedure is well-detailed in equations (13)-(17)

$$v(x,t) = \sum_{n=1}^{\infty} e^{-\hat{k}\lambda_n^2 t}[A_n \cos(\lambda_n x) + B_n \sin(\lambda_n x)] \tag{13}$$

$$\sin \lambda_n L = \sin \sqrt{\frac{\lambda}{\hat{k}}} L = 0$$

Clearly, We have $\lambda_n L = n\pi$, and thus

$$\lambda_n = \frac{n\pi}{L}, \quad n = 1, 2, 3, ..., \tag{14}$$

$$v(x,t) = \sum_{n=1}^{\infty} e^{-\hat{k}\lambda_n^2 t} B_n \sin(\lambda_n x) \tag{15}$$

$$T_0 - \hat{w}(x) = \sum_{n=1}^{\infty} \hat{B}_n \sin(\lambda_n x) \tag{16}$$

$$\begin{aligned} \hat{B}_n &= \frac{2}{L}\int_0^L (T_0 - w(x)) \sin(\lambda_n x) dx \\ &= \frac{2L^2 \dot{f}}{n^3 \pi^3 \hat{k}}[2L^3(\cos(n\pi) - 1)] \end{aligned} \tag{17}$$

Once, both expressions for the punctual steady-state and transient-state temperatures have been obtained, the total average function value (AFV) is obtained following equation (18). The obtained equation will provide the total average temperature throughout the micro-actuator.

$$\Delta T_u = \frac{1}{L}\int_0^L u(x,t)dx - T_0 = \Delta T_w + \Delta T_v \tag{18}$$

Where

$$\Delta T_w = \frac{1}{L}\int_0^L w(x)dx - T_0; \qquad \Delta T_v = \frac{1}{L}\int_0^L x(x,t)dx$$

The AFV of the steady-state part is obtained as (19). Following the same procedure, the AFV of the transient-state is (20). Recalling equation (6), one can write the AFV of the total temperature as (20)

$$\Delta T_w = \frac{1}{12}\frac{\dot{f} L^2}{\hat{k}} \tag{19}$$

$$\Delta T_v = \sum_{n=1}^{\infty} \frac{B_n}{n\pi}[1 - \cos(n\pi)] e^{-\hat{k}\lambda_n^2 t} \tag{20}$$

$$\Delta T_u = \frac{1}{12}\frac{\dot{f} L^2}{\hat{k}} + \sum_{n=1}^{\infty} \frac{B_n}{n\pi}[1 - \cos(n\pi)] e^{-\hat{k}\lambda_n^2 t} \tag{21}$$

To corroborate that the results were correct, an FEM analysis was performed in ANSYS software with the following parameters (See Table 2). The Figure (8a) shows that the proposed model is very close to the FEM solution, variations are attributed to simplifications on the model coupled with corrections that the FEM performs to converge the solution. By analyzing the error, Figure (8b), it is noted that as it happens for most of heat transfer problems (that involve ΔT term) the error is accentuated at early stages due the low value that is being analyzed; as this value increases the error becomes even negligible at a point for later grow again as the system attains the steady-state. This system, from a heat transfer point of view, is satisfactory.

Table 2. V-shaped microactuator parameters

Geometrical			
$W_b(\mu m)$	$t_b(\mu m)$	$W_s(\mu m)$	$t_s(\mu m)$
5	20	10	20
$L_b(\mu m)$	$L_s(\mu m)$	theta ($\theta(deg)$)	m
176	20	5.6	1

Material Properties			
$\rho(\mathrm{kg/m^3})$	$\hat{\rho}(\Omega m)$	$\alpha(K^{-1})$	$C_p(J/KgK)$
2330	$51e^{-6}$	$2.5e^{-6}$	732
k (W/m K)	E (Pa)	U (V)	
156	$160e^{9}$	3	

C. Thermomechanical Modeling

The electrothermal modeling can be related to the thermomechanical modeling with the linear thermal expansion theory. This theory relates the change of a given size as a response to temperature changes.

$$y(t) = \alpha B_1 \Delta T_u - \frac{1}{2mE} B_2 P \tag{22}$$

Where, $B_1 = L_b B^* \sin\theta_b$ and $B_2 = \frac{B^* L_b}{A_b}$ and $B^* = \frac{L_0^2}{w_b^2 \cos^4\theta_b + L_0^2 \sin^2\theta_b}$ are geometrical relations obtained from Castigliano's theorem. α denote the coefficient of thermal expansion (CTE) and Young's modules of the beam material respectively. It must me remarked that the term P account for an external force or disturbance. This term is beyond user's control and for various steps in the analysis it might be set to zero considering the ideal case or to a random value.

From equation (21) and (22)

$$y(t) = \alpha B_1 \left[\frac{1}{12} \frac{\dot{f} L^2}{\hat{k}} + \sum_{n=1}^{\infty} \frac{B_n}{n\pi} [1 - \cos(n\pi)] e^{-\hat{k}\lambda_n^2 t} \right] - \frac{1}{2mE} B_2 P \tag{23}$$

The validation of the thermomechanical modeling is not required given that the relationship between the electrothermal and thermomechanical models is linear, the inclusion of the CTE and E terms resulting in the same behavior but with different magnitudes. As a consequence, the error (%) remains the same.

D. State Space Modeling

The State Space representation can be obtained by differentiating equation (21) with respect to t, to obtain:

$$\Delta \dot{T}_u = -\hat{k} \left[\sum_{n=1}^{\infty} \frac{B_n \lambda_n^2}{n\pi} [1 - \cos(n\pi)] e^{-\hat{k}\lambda_n^2 t} \right] \tag{24}$$

The higher terms of transient expression of ΔT_u are very small compare to its first term of transient expression, hence they can be neglected. Therefore, $\lambda_n = \lambda_1 = \frac{\pi}{L}$.

$$
\begin{aligned}
\Delta\dot{T}_u &= -\hat{k}\lambda_1^2\left[\sum_{n=1}^{\infty}\frac{B_n}{n\pi}[1-\cos(n\pi)]e^{-\hat{k}\lambda_n^2 t}\right] \\
&= -\frac{\hat{k}\pi^2}{L^2}\left[\frac{1}{12}\frac{\dot{f}L^2}{\hat{k}}+\sum_{n=1}^{\infty}\frac{B_n}{n\pi}[1-\cos(n\pi)]e^{-\hat{k}\lambda_n^2 t}-\frac{1}{12}\frac{\dot{f}L^2}{\hat{k}}\right] \\
&= -\frac{\hat{k}\pi^2}{L^2}\Delta T_u+\frac{\pi^2}{12\rho C_p}\frac{A_bA_s}{\hat{\rho}(2L_bA_s+L_sA_b)(A_bL_b+A_sL_s)}U^2
\end{aligned}
\tag{25}
$$

Equations (25) and (22) can be considered as state equation and output equation of a State-Space-Model respectively

$$
\begin{aligned}
\dot{x} &= Ax+Bu \\
y &= Cx+Du
\end{aligned}
\tag{26}
$$

Where,

$$
A=\left[-\frac{\hat{k}\pi^2}{L^2}\right],\quad B=\left[\frac{\pi^2}{12\rho C_p}\frac{A_bA_s}{\hat{\rho}(2L_bA_s+L_sA_b)(A_bL_b+A_sL_s)}\quad 0\right],
$$

$$
C=\left[\alpha B_1\right],\quad D=\left[0\quad \frac{1}{2mE}B_2\right]
$$

$$
x=\left[\Delta T_u\right],\quad u=\begin{bmatrix}U^2\\P\end{bmatrix}
$$

Figure (4) represents the state-space model of the system whereas, figure (5) gives the insight of state-space model. The system combines the electro-thermo-mechanical coupled field modeling which can be decomposed into two sub-models.

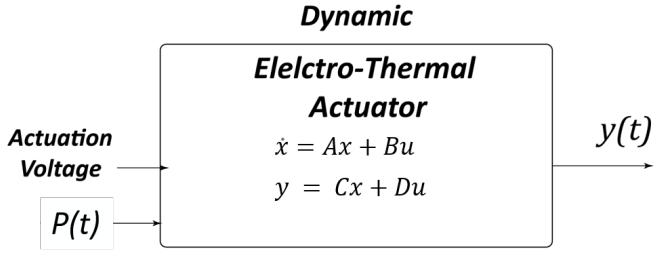

Figure 4. Dynamic Model

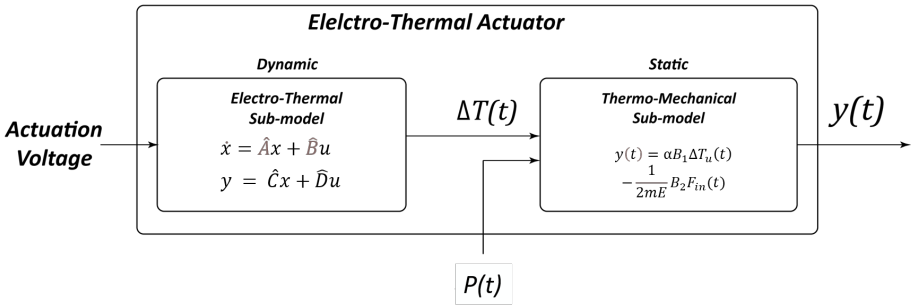

Figure 5. Insight of Dynamic Model

E. Validation of the Approximation

To get the dynamic equation of state space model, an approximation were made to simplify the the equation (24). The higher terms of transient expression of ΔT_u were neglected to get a simplified expression of $\Delta \dot{T}_u$ in equation (25). Figure (6) is a MATLAB plot of $\Delta \dot{T}_u$ from equation (24) and (25). Both curves are indistinguishable, only for very early stages a slight deviation is observed.

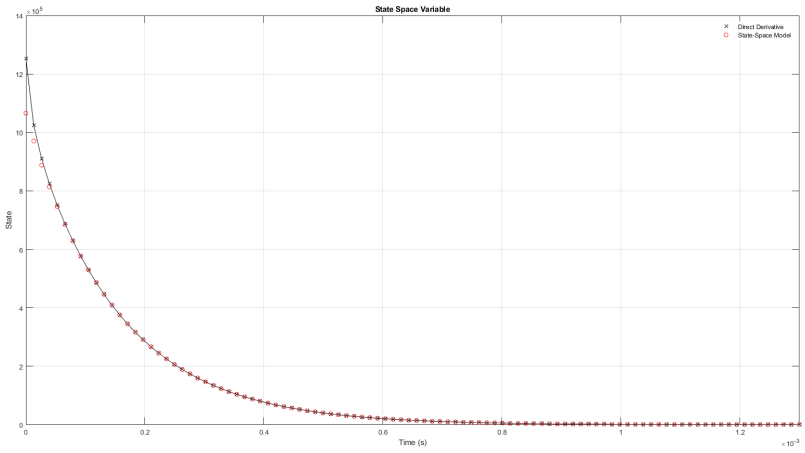

Figure 6. Comparison of the expression of $\Delta \dot{T}_u$ from equation (24) and equation (25) for validation of approximation

III. Controller Design

For the controller design, the $'P'$ term was set to zero assuming that no external forces nor disturbances were acting on the microactuator. This is a valid assumption for most of the cases given that this type of microactuators are utilized under controlled conditions.

A. Controllability and Observability Analysis

Developing the state space model is not of great usefulness if the system cannot be transferred from an initial state to a desired state in a given time (Controllable). The determination of this feature is crucial for any system. The controllability test is based on the rank deficiency of the controllability matrix.[9] If the controllability matrix is full-rank then the system is said to be controllable. The resultant state space representation was proved to be controllable.

By the same token, a system is said to be observable if it can provide the required information to estimate all the states of the system.[9] The observability test is the same as for controllability but applied to the observability matrix. The obtained state-space model is compound by single system (A) and single measurement (C) matrices (See (26)), thus the system is inherently Observable.

B. Linear Quadratic Regulation Controller

The linear quadratic regulation (LQR) controller is one of the most influential methods within the controls field. It is a well-known design technique that provides appropriate feedback gains. LQR controllers have linear feedback gains which simplify considerably its analysis and its implementation, not to mention the good disturbance rejection and tracking that it offers.[10] Selecting the weighting matrices (Q,R) is crucial for the performance of the controller, these weighting matrices can be calculated using the weighting constants depending on the designer's preferences.

1. Control Gain Development

For the demonstration, it is assumed that the control object is to control displacement will 3 times lesser time than the natural response. The values of Q and R were selected arbitrarily and then tweaked by hit and trial, which came out to be 1 for the results shown. Using the $lqr()$ function in MATLAB, the LQR feedback gain was computed

to be 0.9069 and the feed-forward gain was computed to be 1.0048. These parameters were used for the controller simulation.

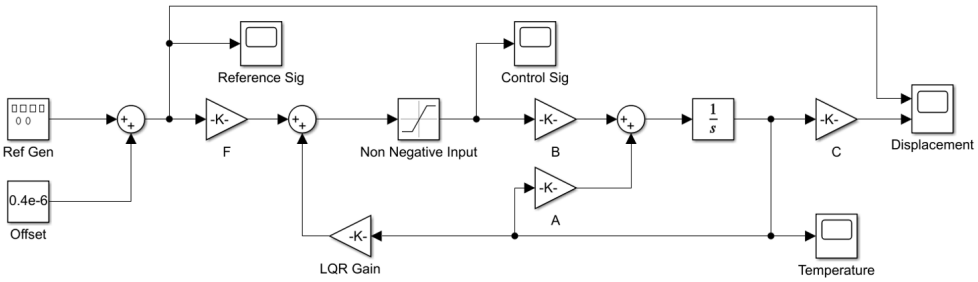

Figure 7. Simulink Block Diagram

IV. Results and Discussion

A. Validation of State-Space Dynamic Model

To validate the state-space dynamic model, the step response of the system taken from MATLAB were compared with the step response of the system taken from FEM. Figure (8a) shows the comparison between step response of the system from two different method of analysis. Whereas, figure (8b) demonstrate the deviation of step response of the system taken from MATLAB with respect to the step response of the system taken from FEM in time. Except for few milliseconds in the beginning, the error does not exceed 5%.

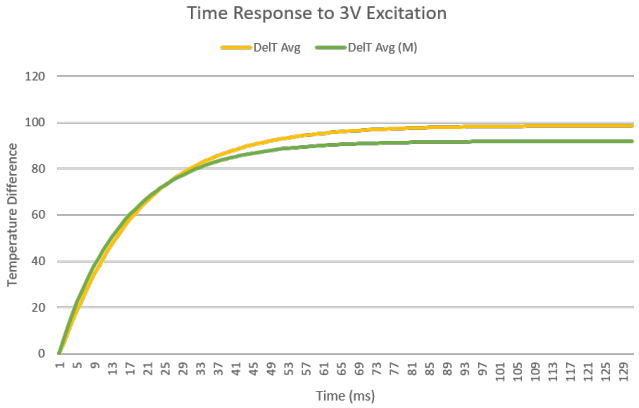

(a) FEM vs our Model

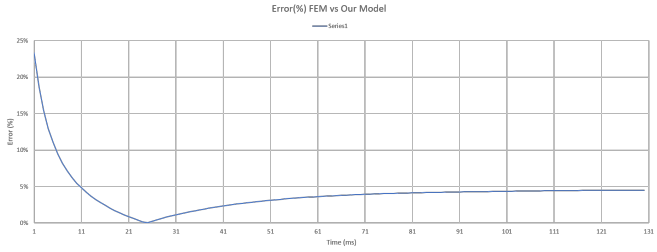

(b) Error (%) with time

Figure 8. (a) FEM vs our Model, (b) Error (%) with time

B. Simulink Results

The state space model developed was programmed in MATLAB Simulink using Controls Toolbox. Using the LQR feedback gain and the forward gains, already calculated, the feedback controller was also implemented on the system. As shown in the state space model, the input to the system is actually voltage squared, but not the voltage. This means, that the positive and negative voltage will have the same expansion and same output. Negative value of voltage squared is non-existent in physics. This implies that the dynamic system cannot take any negative control input. Generally, LQR controller does not incorporate such physical limitations of the system, so using a saturation block in Simulink, the control signal is saturated for any values less than zero. Fig. 7 shows the block diagram of the Simulink program. This program can be used to see the simulated output time response for any reference input. Fig. 9 shows the tracking results for different input references. The reference is shown in blue while the simulated output of the system is shown in red. The control signal calculated by LQR controller is also shown in sub-figures. The affect of saturation of negative input can be seen in (b) and (c).

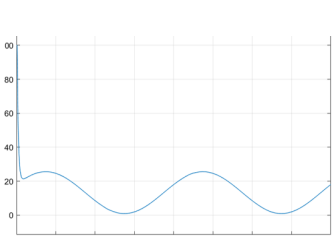

(a) Control Signal for (d)

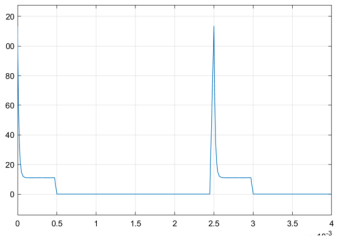

(b) Control Signal for (e)

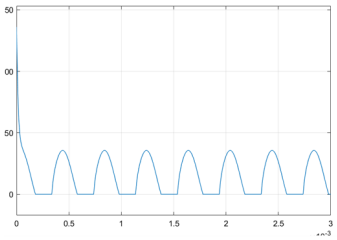

(c) Control Signal for (f)

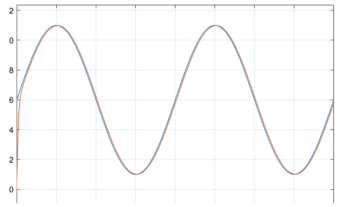

(d) Simulated output response for 500 Hz sinusoidal

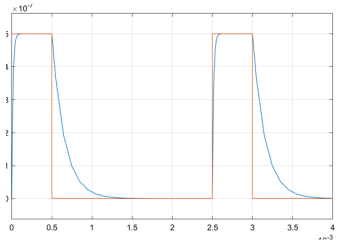

(e) Simulated output response for step input

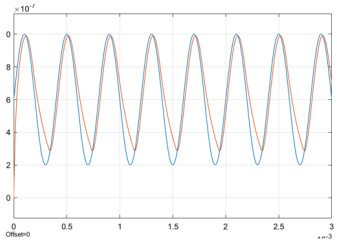

(f) Simulated output response for 1500 Hz sinusoidal

Figure 9. Simulink Results

V. Conclusion

For the first time, a state space dynamic model of the V-shaped electrothermal microactuator is developed, while taking reaction force and voltage difference as an output. Incorporating reaction force, makes the model useful in applications where an environment interaction is required for the MEMS device. The dynamic model is verified by Finite Element Method, and it is shown that the developed model coincides with the natural step response of the system in FEM. A controller design methodology is developed, along with its demonstration on a selected microactuator with specified dimensions and MUMPS based material. The designed controller showed 300 percent faster response of the microactuator. Dynamic modelling of the actuator will give new opportunities to the MEMS researchers to use this actuator for biomedical applications especially, stiffness characterization, and gyroscopes where higher frequency response is required. The analysis of the dynamic model shows that cooling is an uncontrolled phenomenon and no control input can be used for this operation. Further studies must have to be done so as to improve the frequency response by changing the design and geometry.

References

[1]Judy, J. W., "Microelectromechanical systems (MEMS): fabrication, design and applications," *Smart Materials and Structures*, Vol. 10, No. 6, 2001, pp. 1115â1134.

[2]Bao, M. and Wang, W., "Future of microelectromechanical systems (MEMS)," *Sensors and Actuators A: Physical*, Vol. 56, No. 1-2, 1996, pp. 135â141.

[3]Fujita, H., "Microactuators and micromachines," *Proceedings of the IEEE*, Vol. 86, No. 8, Aug 1998, pp. 1721â1732.

[4]Popa, D., "Microactuators," *Encyclopedia of Microfluidics and Nanofluidics*, 2008, pp. 1100â1103.

[5]Tabib-Azar, M., *Microactuators: electrical, magnetic, thermal, optical, mechanical, chemical smart structures*, Kluwer, 1998.

[6]Denishev, K. and Krumova, E. Z., *ELECTRONICSâ 2005*.

[7]Chen, H., Wang, X.-J., Wang, J., and Xi, Z.-W., "Analysis of the dynamic behavior of a V-shaped electrothermal microactuator," *Journal of Micromechanics and Microengineering*, Vol. 30, No. 8, 2020, pp. 085005.

[8]Zhang, Z., Zhang, W., Wu, Q., Yu, Y., Liu, X., and Zhang, X., "Closed-form modelling and design analysis of V- and Z-shaped electrothermal microactuators," Nov 2016.

[9]Preumont, A., *Vibration Control of Active Structures*, Kluwer Academic Publishers, 1997.

[10]Hudson, M. and Reynolds, P., "Implementation considerations for active vibration control in the design of floor structures," *Engineering Structures*, Vol. 44, 2012, pp. 334â358.